

Symposium on the Application
of Mechanics to Geophysics
Scripps Institute of Oceanography,
University of California at San Diego
17 and 18 January 2015

***Shear localization due to thermal pressurization
of pore fluids in rapidly sheared granular media***

James R. Rice (*Harvard Univ.*)

Collaborators:

John D. Platt (*Carnegie Institution, Washington*)

John W. Rudnicki (*Northwestern Univ.*)

Nicolas Brantut (*Univ. College London*)

Abstract

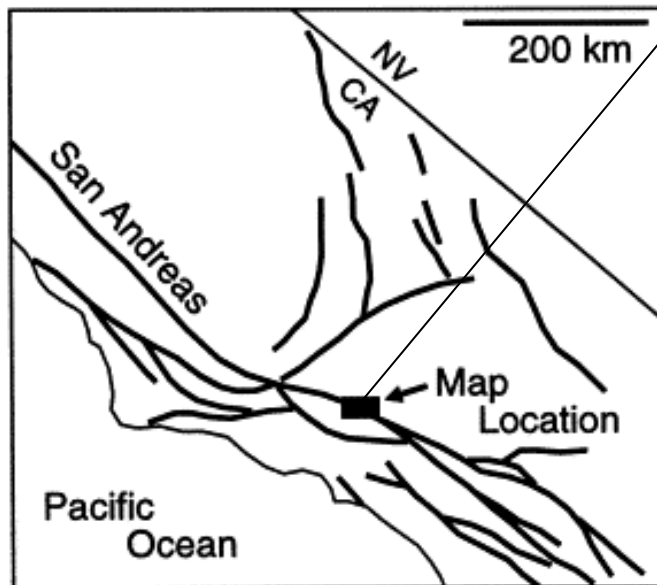
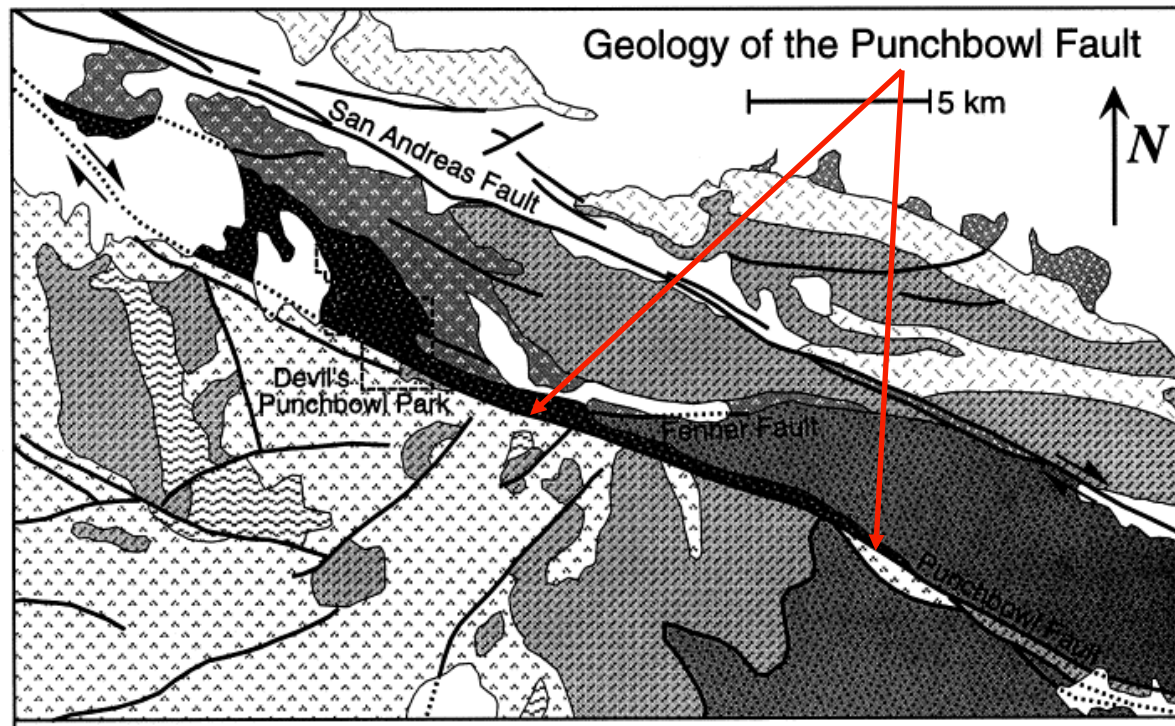
Field observations of mature, well-slipped, earthquake fault zones show that the majority of shear is often localized to principal slipping zones of order 10-100 mm width within a broader gouge layer of order 10-100 mm wide (with all that being a feature locating within a much broader, 1-10s m wide, damage zone bordering the fault). Such fault gouges are often rate-strengthening, especially at higher temperatures, and are then resistant to shear localization under slow deformation.

We show that extreme localization is, instead, a predicted consequence of rapid straining, with related shear heating, of fluid-infiltrated gouge on time scales that are too short for significant pore-fluid drainage or heat conduction. The localization is due to development of highly elevated pore pressure, hence of lowered Terzaghi effective stress, from thermal expansion of the fluid (i.e., thermal pressurization of the pore fluid, when expansion is constrained by a low-permeability host).

Results are presented for two versions of the process: In the classical one, the pore fluid pre-exists in the gouge as groundwater. In another, the study of which was pioneered by J. Sulem and co-workers, thermal decomposition reactions in hydrated silicates (clays, serpentines) or carbonates within gouge are triggered as temperature rises, releasing as volatile a fluid phase (H₂O or CO₂) at high pressure.

Some of the work is published in JGR in 2014 (doi: 10.1002/2013JB010710 and 010711) and some is in review there as of early 2015.

Chester & Chester
[*Tectonophys.*, 1998]



Earthquake shear is highly localized

Punchbowl PSS, composite based on Chester & Chester [*Tectonophysics* '98] & Chester & Goldsby [*SCEC* '03]

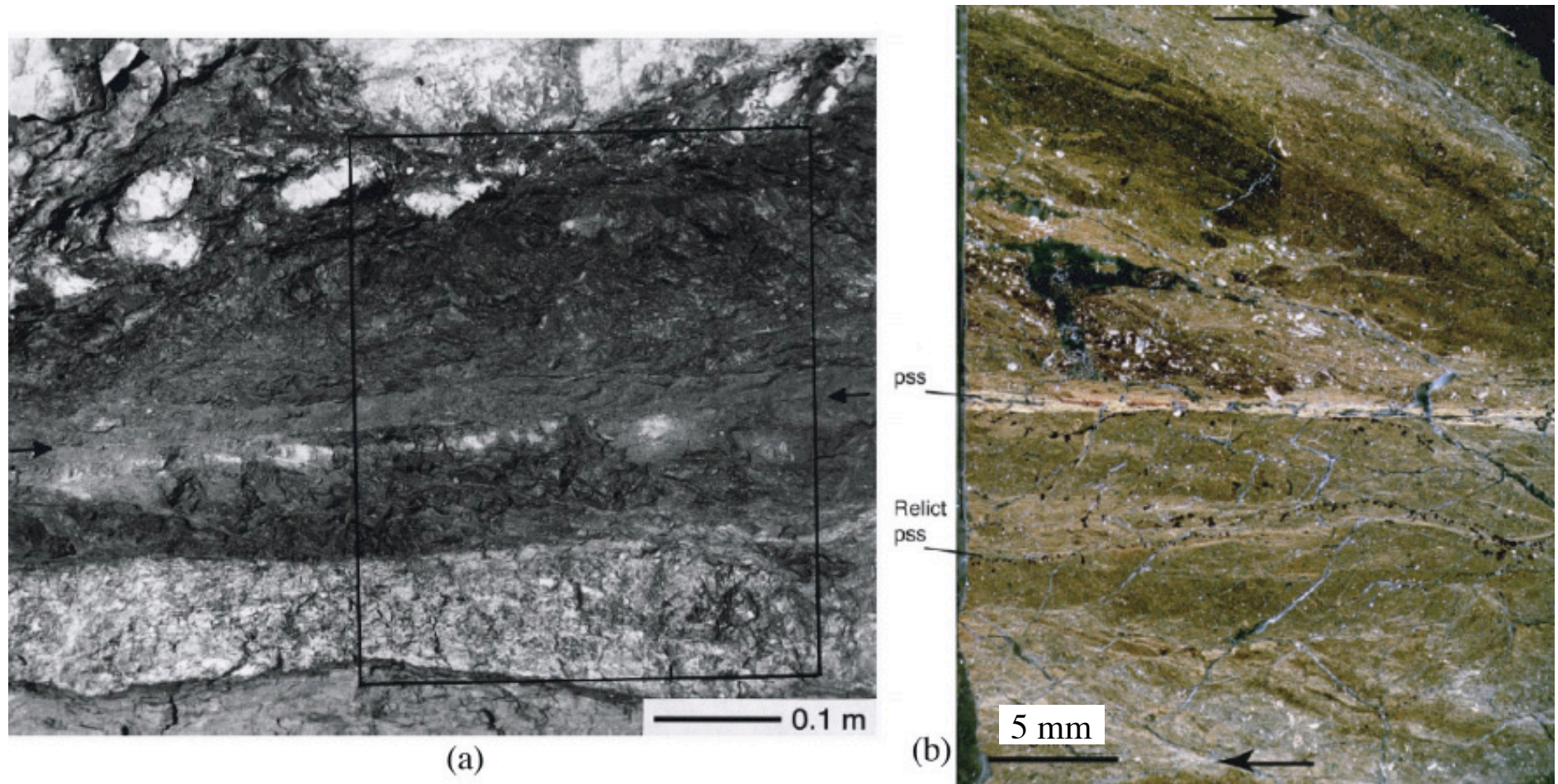
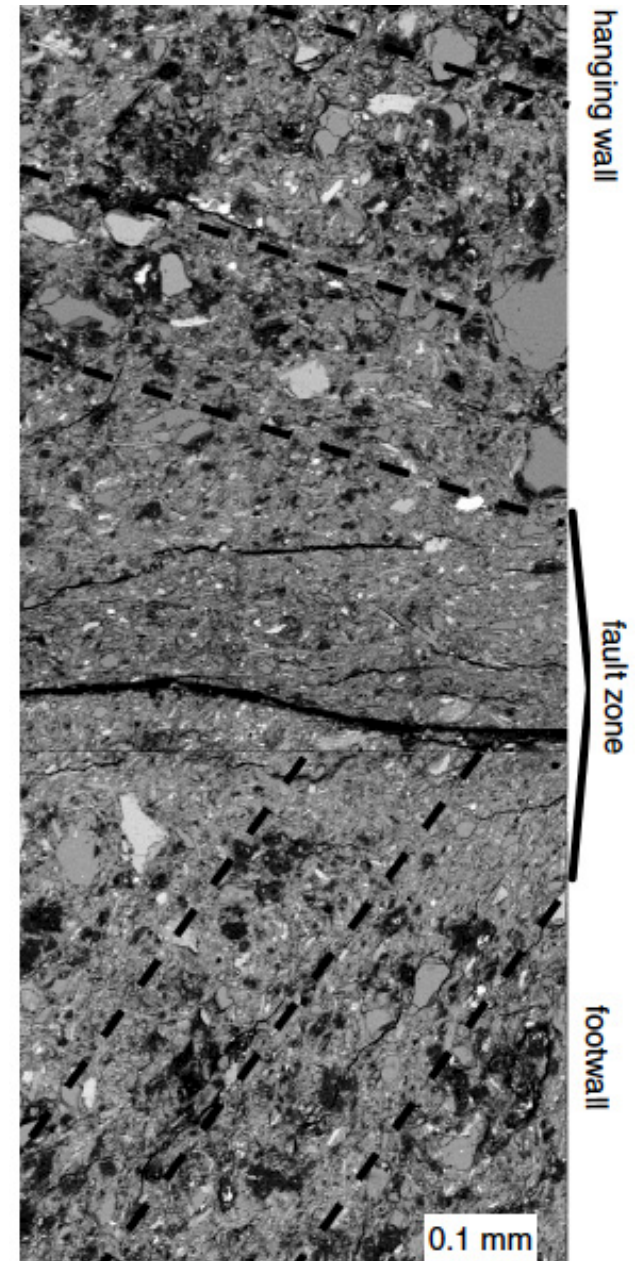
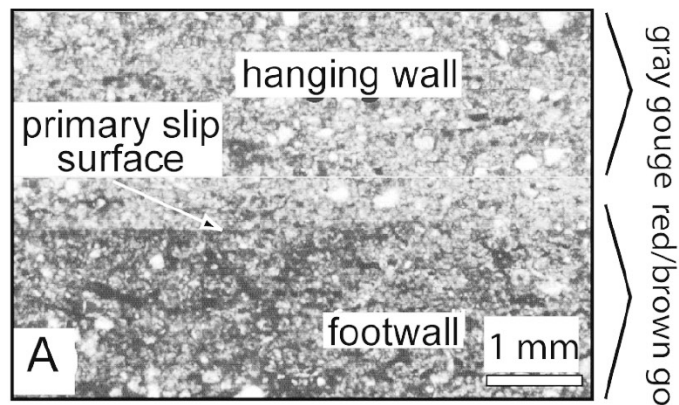
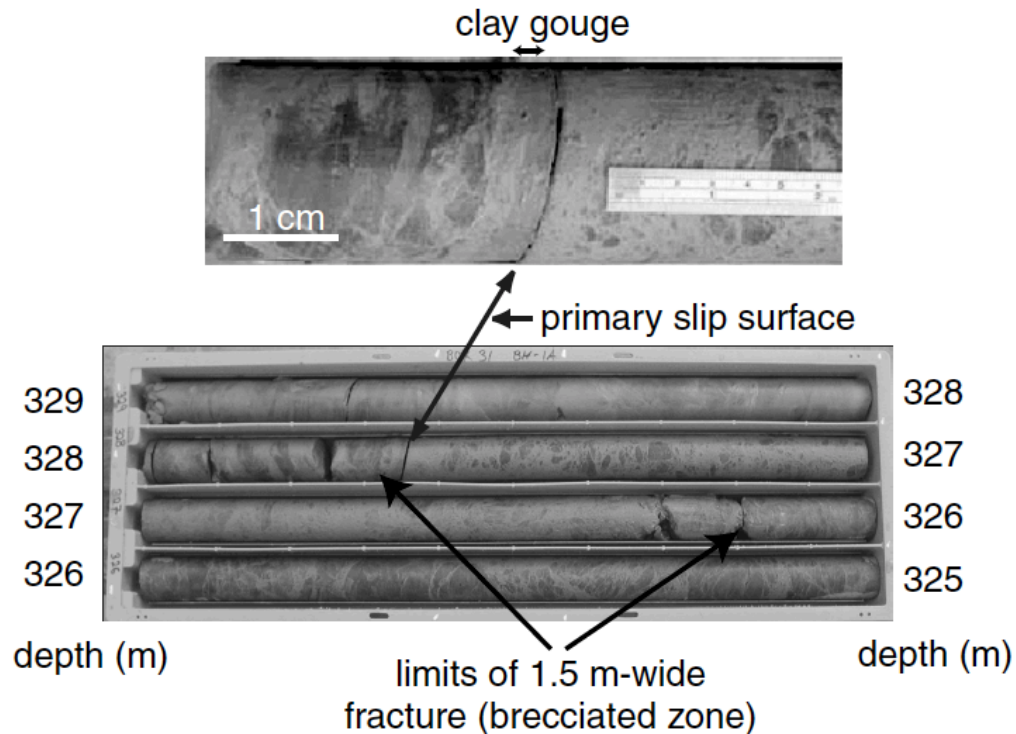


Figure 1. Principal slip surface (PSS) along the Punchbowl fault. (a) From *Chester and Chester* [1998]: Ultracataclasite zone with PSS marked by black arrows; note 100 mm scale bar. (b) From Chester et al. (manuscript in preparation, 2005) [also *Chester et al.*, 2003; *Chester and Goldsby*, 2003]: Thin section; note 5 mm scale bar and ~ 1 mm localization zone (bright strip when viewed in crossed polarizers due to preferred orientation), with microshear localization of most intense straining to $\sim 100\text{--}300\text{ }\mu\text{m}$ thickness.

[Heermance, Shipton & Evans, *BSSA*, 2003]

Core retrieved across the Chelungpu fault, which hosted the 1999 Mw 7.6 Chi-Chi, Taiwan, earthquake: Suggests slip at 328 m depth traverse was accommodated within a zone ~ 50–300 μm thick.

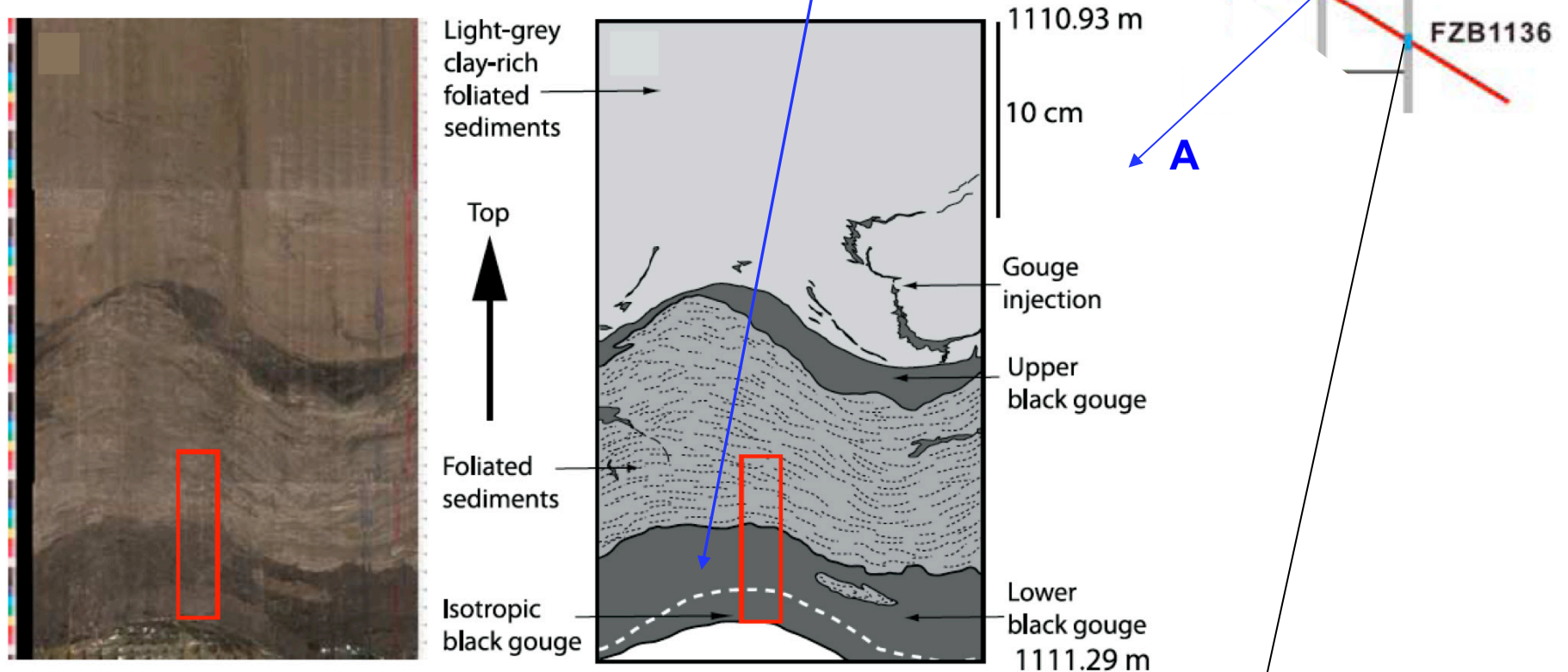


Two other Chelungpu Fault, Taiwan boreholes

[Boullier et al., GGG 2009, GSL 2011]:

Principal Slip Zone (PSZ) localized within black gouges

- **Hole A, fault at 1111 m depth: PSZ is ~2 cm thick**



Unrolled scanning image of FZA1111 and corresponding sketch

- **Hole B, fault at 1136 m depth: PSZ is ~3 mm thick**

PSZ layering defined by variations in concentrations of clay minerals and clasts, comparable to structures produced in high-rate rotary shear experiments.

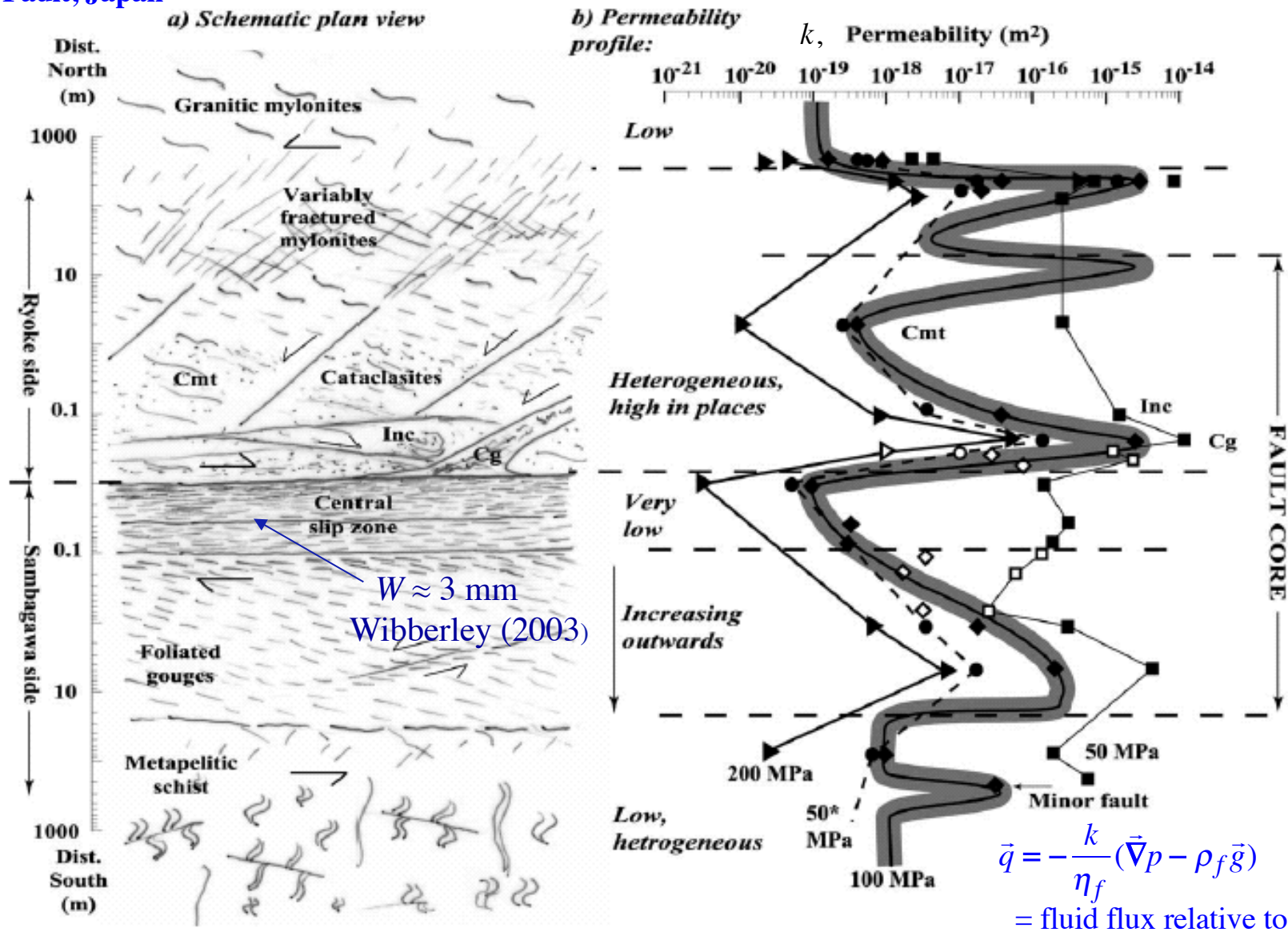


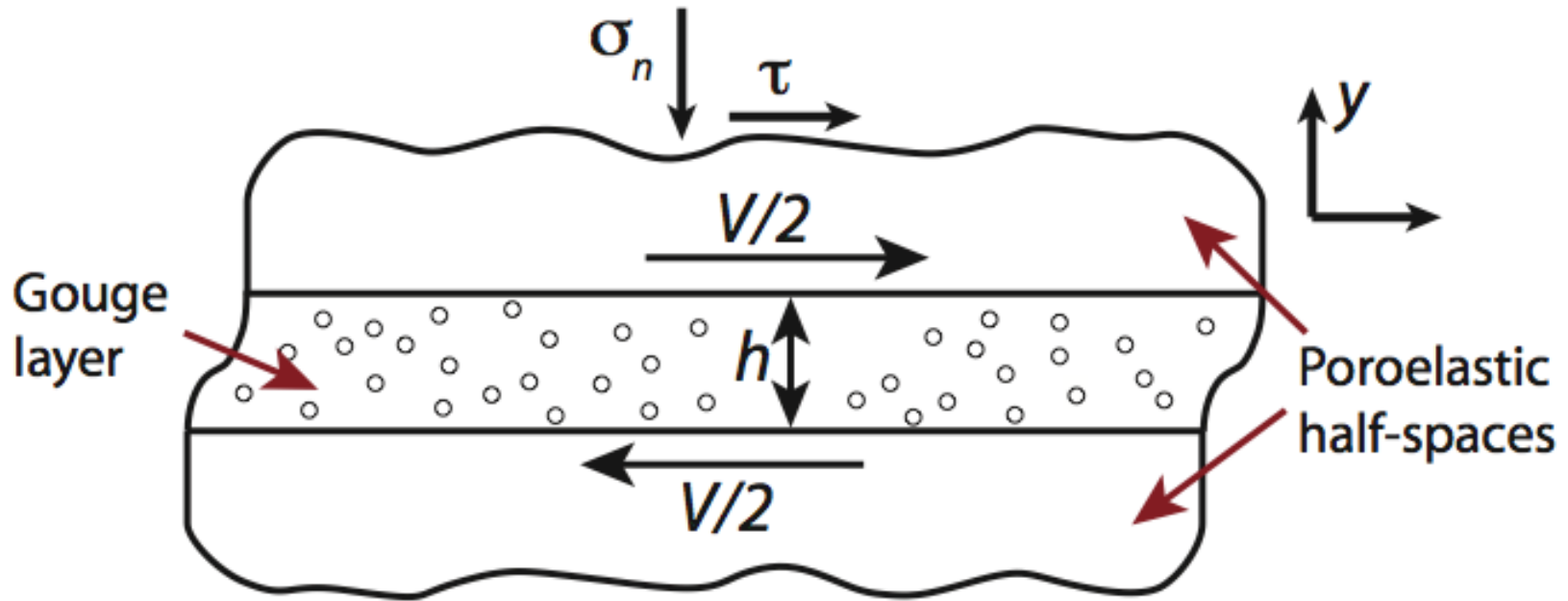
Fig. 11. Sketch summary of the main elements of permeability structure across the Median Tectonic Line. (a) Summary of the structural zones; (b) summary permeability data distribution for different confining pressures (stated at the base, with * denoting data from the deconfining path), for 20 MPa pore pressure, given the mapped distribution of fault rocks shown in Figs. 1–3. Note that the distance axis is logarithmic in both directions away from the Ryoke/Sambagawa contact. 'Cmt' and 'Inc' denote cemented and incohesive foliated cataclasites, respectively, and 'Cg' denotes crenulated gouge.

$$\tau = f \times (\sigma_n - p)$$

Statically strong but dynamically weak faults, e.g., due to thermal weakening in rapid, large slip:

- *Process expected to be important from start of seismic slip:*
 - Thermal pressurization of in-situ pore fluid, reduces effective stress.
- *Process that may set in at large enough rise in T :*
 - Thermal decomposition, fluid product phase at high pressure (e.g., CO_2 from carbonates; H_2O from clays or serpentines).
- *Ultimately:*
 - Melting at large slip, if above have not limited increase of T .

Shear of a fluid-saturated gouge layer



- Two non-yielding half-spaces are moved relative to each other at a speed V .
- All inelastic deformation accommodated in gouge layer, leading to a nominal strain rate $\dot{\gamma}_0 = V / h$.

Thermo-mechanical model in gouge layer

- To model the deforming gouge layer we use,

Mechanical equilibrium $\frac{\partial \tau}{\partial y} = 0, \quad \frac{\partial \sigma_n}{\partial y} = 0$

Conservation of energy $\frac{\partial T}{\partial t} - \alpha_{th} \frac{\partial^2 T}{\partial y^2} = \frac{\tau \dot{\gamma}}{\rho c}$

Conservation of fluid mass $\frac{\partial p}{\partial t} - \alpha_{hy} \frac{\partial^2 p}{\partial y^2} = \Lambda \frac{\partial T}{\partial t}$

- Shear stress modeled using the effective stress and **rate-strengthening** friction,

$$\tau = f(\dot{\gamma})(\sigma_n - p) \quad f(\dot{\gamma}) = f_0 + (a - b) \log \left(\frac{\dot{\gamma}}{\dot{\gamma}_0} \right)$$

(We assume $a - b \equiv (\dot{\gamma} df(\dot{\gamma}) / d\dot{\gamma})_{\dot{\gamma}=\dot{\gamma}_0} > 0$)

Shear between moving rigid blocks of perfectly insulating, impermeable material :

Exact homogeneous shear solution (Lachenbruch, JGR, 1980, version ignoring dilatancy) :

$$\tau(t) = f_o (\sigma_n - p(t)) = f_o (\sigma_n - p_a) \exp \left(-f_o \frac{\Lambda}{\rho c} \dot{\gamma}_o t \right),$$

$$(\dot{\gamma}_o = V / h)$$

Linearized perturbation analysis :

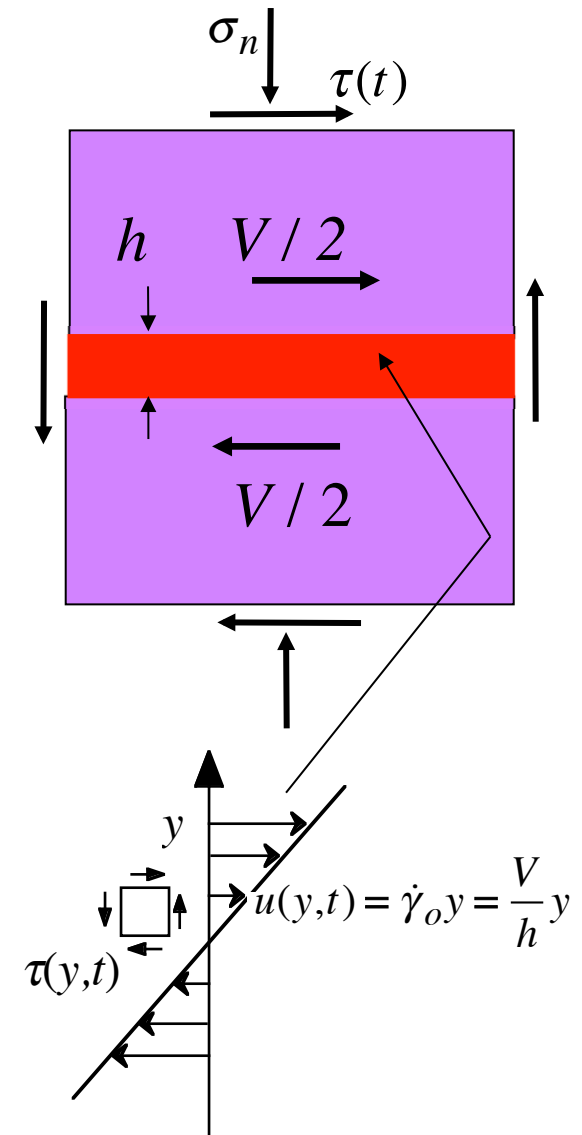
Is that solution stable to small perturbations?

Not unless h is very small !

$$\text{Stable only if } h \leq W_{crit} \equiv \frac{\pi^2}{\left(2 + \frac{f_o}{a-b}\right)} \frac{\rho c}{f_o \Lambda} \frac{(\alpha_{th} + \alpha_{hy})}{V}.$$

$$\left(\text{Typically, } \frac{f_o}{a-b} \gg 2 \Rightarrow W_{crit} \approx \pi^2 \frac{a-b}{f_o^2} \frac{\rho c}{\Lambda} \frac{\alpha_{th} + \alpha_{hy}}{V} \right)$$

[$W_{crit} = \lambda_{shr} / 2$, where λ_{shr} = longest wavelength λ for stable linearized response to infinitesimal $\exp(2\pi i y / \lambda)$ perturbation]



Rice, Rudnicki & Platt
(JGR 2014)

Estimates of maximum stable shear layer thickness (i.e., localized zone width) W_{crit}

Results, using $f_o = 0.4$, $\frac{f_o}{a-b} = 20$, $V = 1 \frac{\text{m}}{\text{s}}$, $\alpha_{th} = 0.7 \frac{\text{mm}^2}{\text{s}}$, $\rho c = 2.7 \frac{\text{MPa}}{^\circ\text{C}}$:

Corresponding to ~ 7 km depth :

Low estimate (Based on lab properties of *intact* Median Tectonic Line gouge [Wibberley and Shimamoto, 2003] at effective confining stress = 125 MPa and $T = 200^\circ\text{C}$):

$$\Lambda = 0.70 \frac{\text{MPa}}{^\circ\text{C}}, \text{ and } \alpha_{hy} = 1.5 \frac{\text{mm}^2}{\text{s}} \Rightarrow \boxed{W_{crit} = 3-5 \mu\text{m}}$$

High estimate (Accounts very roughly for *fresh damage* of the initially intact fault gouge, introduced at the rupture front just before and during shear, by increasing permeability k to $k^{dmg} = 5-10 k$, and increasing drained compressibility β_d to $\beta_d^{dmg} = 1.5-2 \beta_d$):

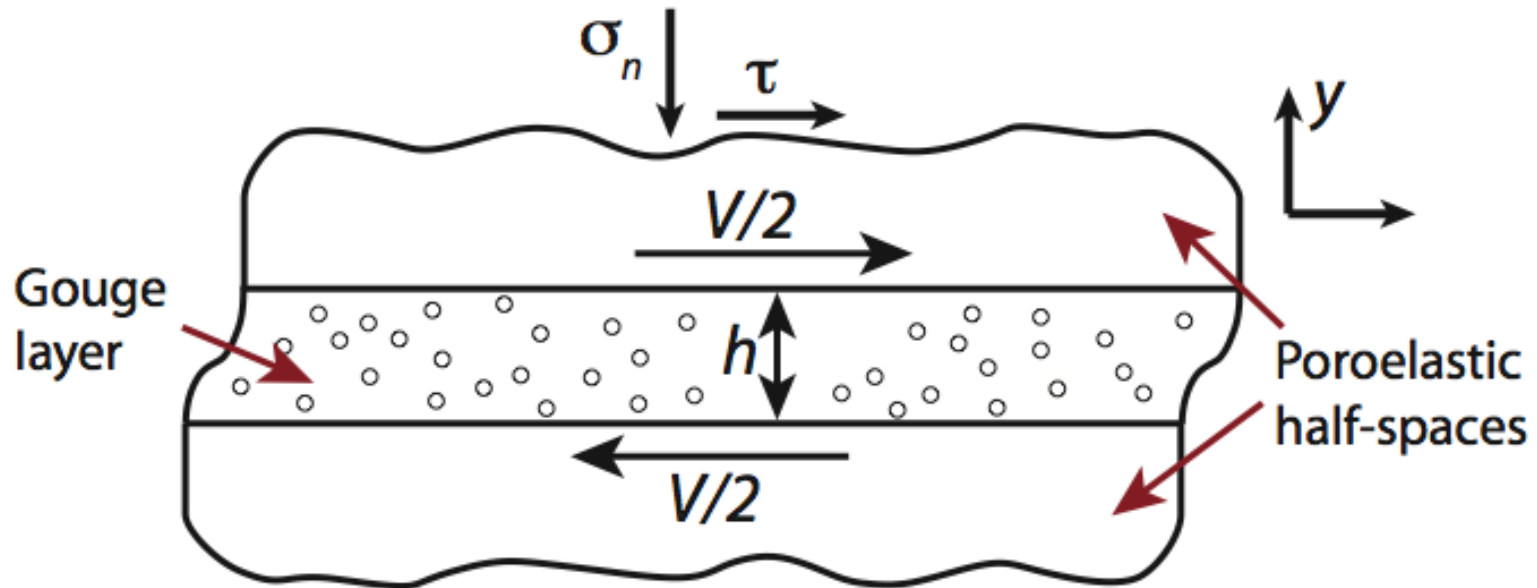
$$\Lambda \approx 0.34 \frac{\text{MPa}}{^\circ\text{C}}, \text{ and } \alpha_{hy} \approx 3.5 \frac{\text{mm}^2}{\text{s}} \Rightarrow \boxed{W_{crit} \approx 25-40 \mu\text{m}}$$

Corresponding to ~ 1 km depth :

Low estimate : $\boxed{W_{crit} \sim 25 \mu\text{m}}$

High estimate : $\boxed{W_{crit} \sim 200 \mu\text{m}}$

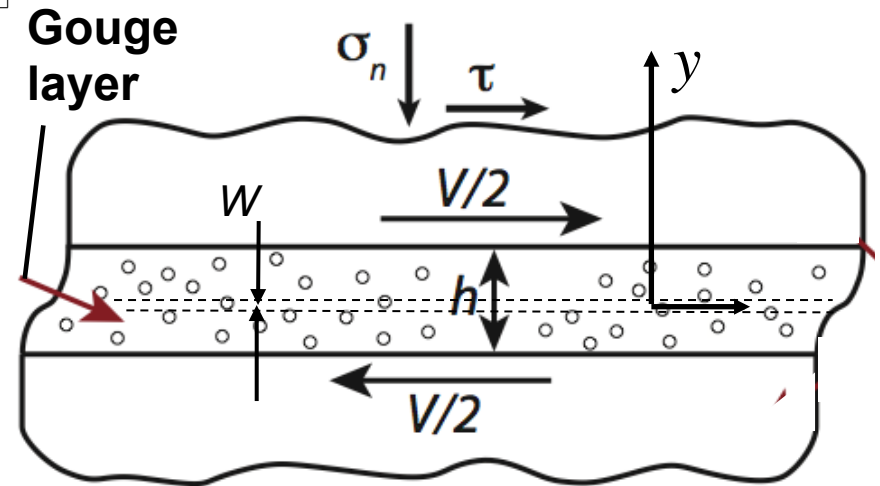
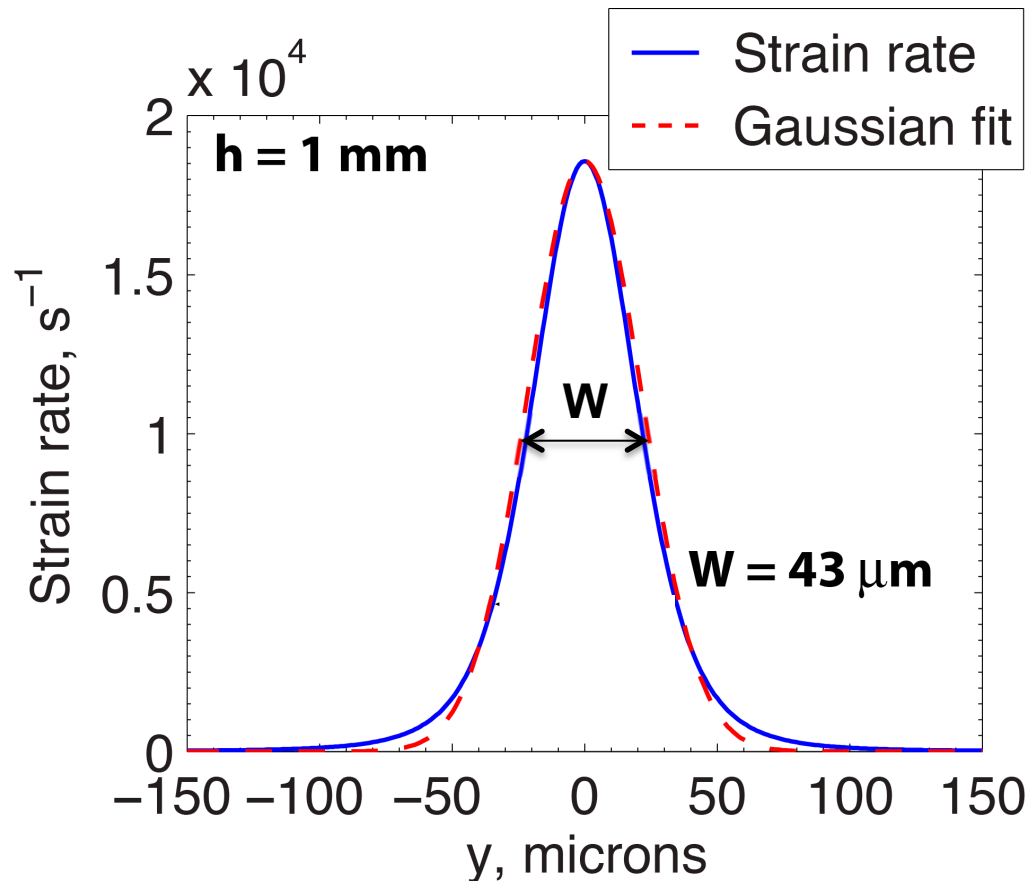
Shear of a fluid-saturated gouge layer:
Full nonlinear numerical solutions
(vs. linearized perturbations)



- Two non-yielding half-spaces are moved relative to each other at a speed V (taken as 1 m/s).
- All deformation accommodated in gouge layer leading to a nominal strain rate, $\dot{\gamma}_o = \frac{V}{h}$

Strain localization

- Simulations using representative physical values show that strain localization does occur.



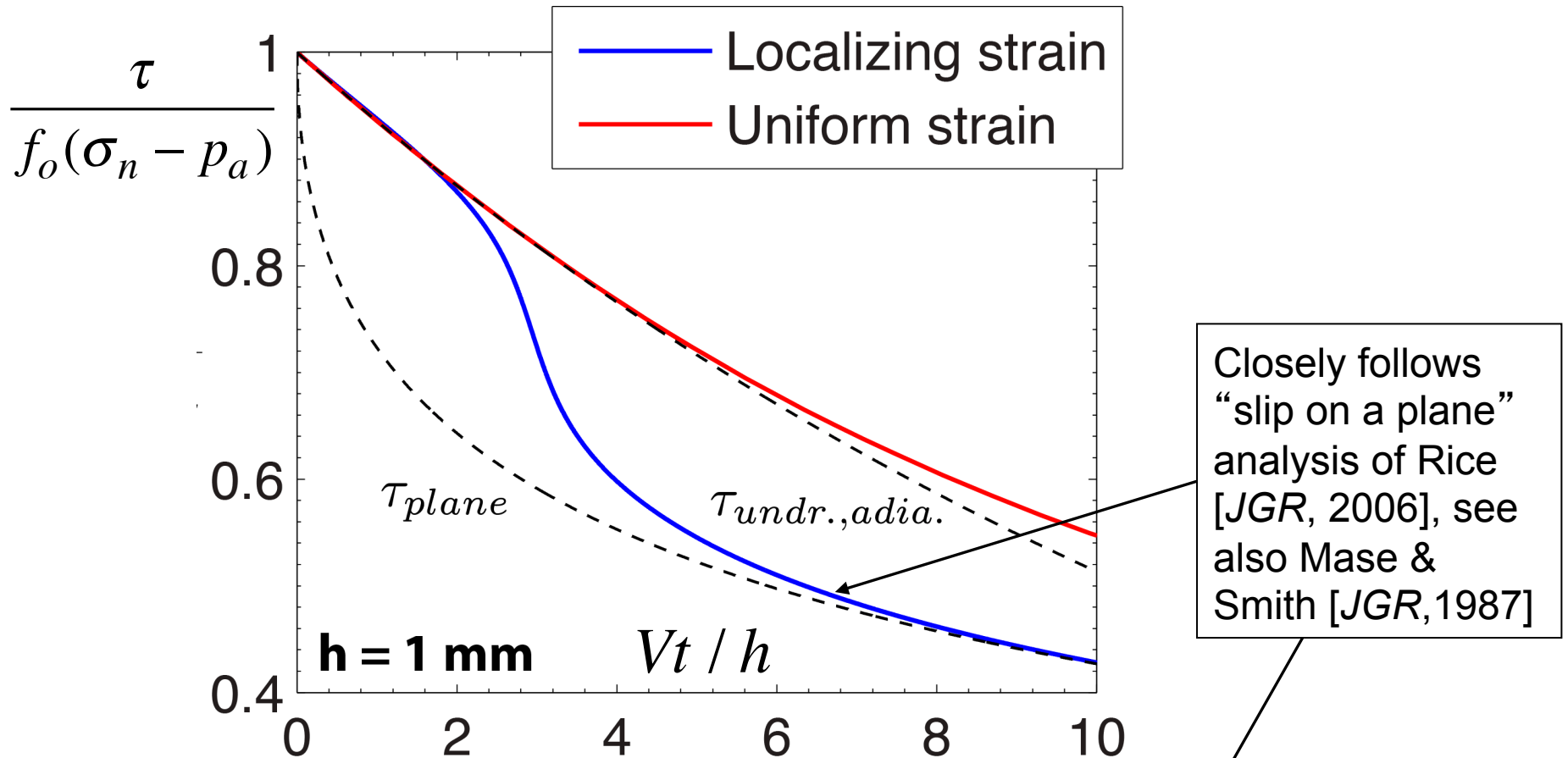
- Deformation has localized to a zone much thinner than the layer, $W \ll h$ ($43 \mu\text{m} \ll 1,000 \mu\text{m}$).

$W_{\text{nonlin. calc.}}$ is comparable to $W_{\text{lin. pert.}}$.

Implications, dynamic weakening

Platt, Rudnicki
& Rice (JGR 2014)

- Weakening of the gouge layers during localization



- Localization leads to additional weakening.

$$\tau = f_o(\sigma_n - p_a) \exp\left(\frac{Vt}{L^*}\right) \operatorname{erfc}\left(\sqrt{\frac{Vt}{L^*}}\right) \quad \text{where} \quad L^* = \left(\frac{2\rho c}{f_o\Lambda}\right)^2 \frac{(\sqrt{\alpha_{hy}} + \sqrt{\alpha_{th}})^2}{V}$$

$$\tau = f \times (\sigma_n - p)$$

Statically strong but dynamically weak faults, e.g., due to thermal weakening in rapid, large slip:

- *Process expected to be important from start of seismic slip:*
 - Thermal pressurization of in-situ pore fluid, reduces effective stress.
- *Process that may set in at large enough rise in T :*
 - Thermal decomposition, fluid product phase at high pressure (e.g., CO_2 from carbonates; H_2O from clays or serpentines).
- *Ultimately:*
 - Melting at large slip, if above have not limited increase of T .

Examples, thermal decomposition:

Dolomite, $\text{CaMg}(\text{CO}_3)_2$ (De Paola et al., *Tectonics*, 2008, *Geology*, 2011; Goren et al., *J. Geophys. Res.*, 2010):

- At $T \sim 550^\circ\text{C}$, dolomite decomposes to calcite, periclase, and carbon dioxide:
$$\text{CaMg}(\text{CO}_3)_2 \rightarrow \text{CaCO}_3 + \text{MgO} + \text{CO}_2$$
- At $T \sim 700\text{-}900^\circ\text{C}$, the calcite further decomposes to lime and carbon dioxide:
$$\text{CaCO}_3 \rightarrow \text{CaO} + \text{CO}_2$$

Many clays and hydrous silicates (Brantut et al., *J. Geophys. Res.*, 2010):

- At $T \sim 500^\circ\text{C}$ ($\sim 300^\circ\text{C}$ for smectite, $\sim 800^\circ\text{C}$ for chlorite), decomposition releasing H_2O starts.

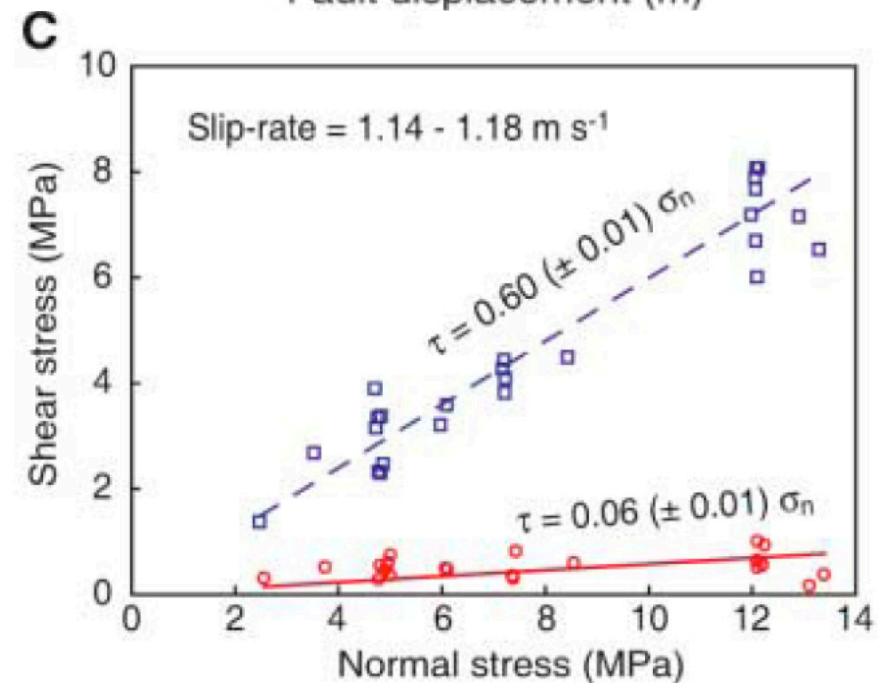
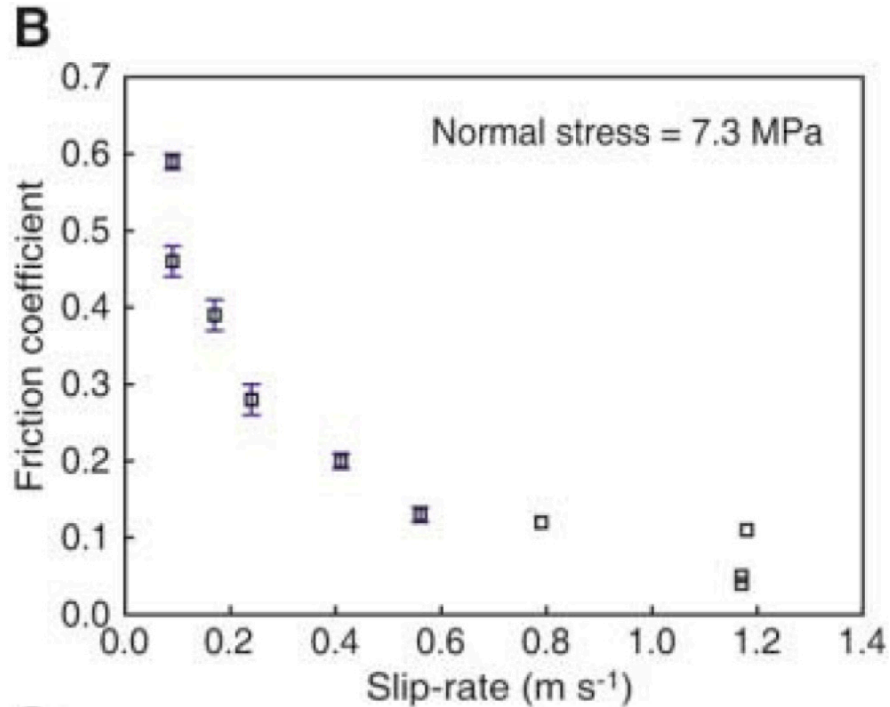
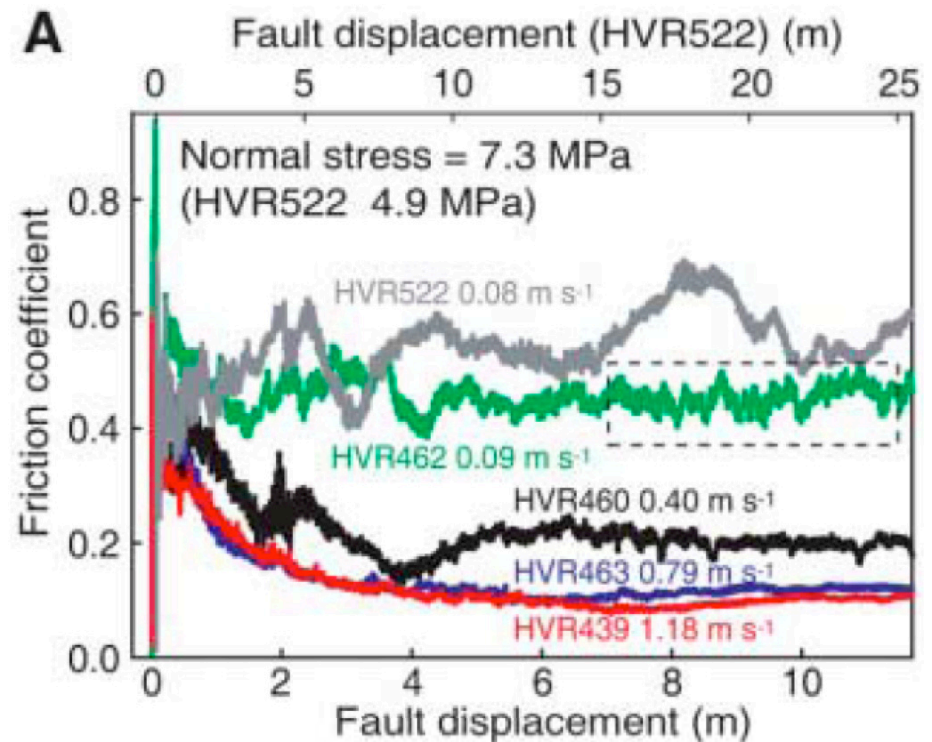
Gypsum, $\text{CaSO}_4(\text{H}_2\text{O})_2$ (Brantut et al., *Geology*, 2010):

- At $T \sim 100^\circ\text{C}$, gypsum dehydrates to form bassanite:
$$\text{CaSO}_4(\text{H}_2\text{O})_2 \rightarrow \text{CaSO}_4(\text{H}_2\text{O})_{0.5} + 1.5 \text{H}_2\text{O}$$
- At $T \sim 140^\circ\text{C}$, bassanite turns into anhydrite
$$\text{CaSO}_4(\text{H}_2\text{O})_{0.5} \rightarrow \text{CaSO}_4 + 0.5 \text{H}_2\text{O}$$

[Han, Shimamoto, Hirose, Ree & Ando, *Sci.*, 2007]:

Carbonate Faults

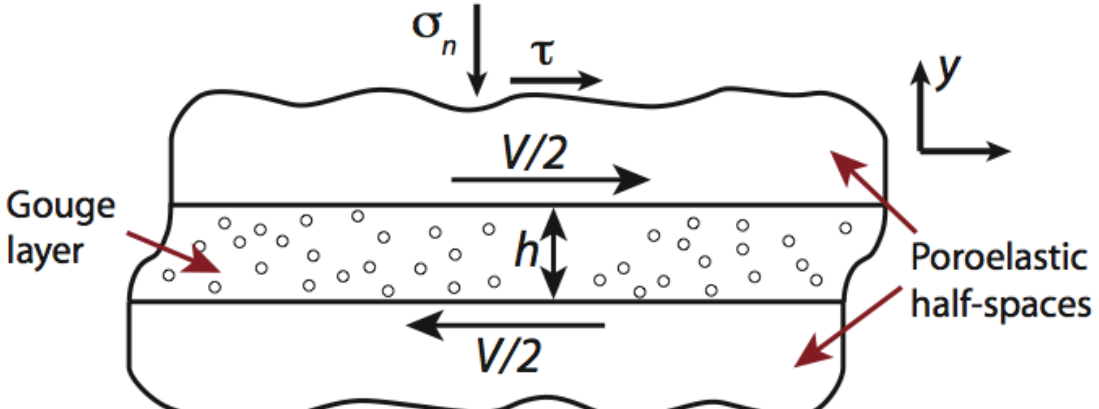
Simulated faults in Carrara Marble at subseismic to seismic slip rates)



Model for decomposing gouge material

- To model the deforming gouge layer we use, based on J. Sulem and co-workers (Vardoulakis, Brantut, Ghabezloo, Famin, Lazar, Noda, Schubnel, Stefanou, Veveakis, ...),

$$\frac{\partial T}{\partial t} = \frac{\tau \dot{\gamma}}{\rho c} + \alpha_{th} \frac{\partial^2 T}{\partial y^2} - E_r \frac{\partial \xi}{\partial t}$$

$$\frac{\partial p}{\partial t} = \Lambda \frac{\partial T}{\partial t} + \alpha_{hy} \frac{\partial^2 p}{\partial y^2} + P_r \frac{\partial \xi}{\partial t}$$


The diagram illustrates a mechanical model of a fault gouge layer. A central horizontal layer, labeled 'Gouge layer', has a thickness h and contains numerous small circles representing pores. This layer is sandwiched between two 'Poroelastic half-spaces'. A normal stress σ_n is applied vertically downwards at the top surface, while a shear stress τ is applied horizontally to the right. The shear velocity on both the top and bottom interfaces is denoted as $V/2$, with arrows pointing in opposite directions. A coordinate system is defined on the right with a vertical y -axis pointing upwards and a horizontal x -axis pointing to the right.

- We assume that the reaction follows an Arrhenius kinetic law,

$$\frac{\partial \xi}{\partial t} = A(1 - \xi) \exp\left(-\frac{Q}{RT}\right) \quad (\text{which allows for } \textit{depletion})$$

Table 2. List of reaction parameters.

Platt, Brantut & Rice (in review 2015 for *JGR*)

Parameter	Decarbonation reaction	Dehydration reactions		
	Calcite ^a	Lizardite ^b	Illite/muscovite ^c	Talc ^d
Pre-exponential factor, $\log_{10}(A)$ (A in 1/s)	15.47	17.80	6.92	14.30
Activation energy, Q (kJ/mol)	319	328	152	372
Fluid mass, $m_{tot}^{100\%}$ (kg/m ³),	1140	240	150	131
Enthalpy ^e , ΔH (MJ/kg)	7.25	2.56	5.49	5.17
Solid volume change, ϕ ($\times 10^{-3}$ m ³ /kg)	0.46	0.88	0.35	0.78
Fluid density, ρ_f (m ³ /kg)	418	267	135	159
T_r	960 °C	885 °C	1733 °C	1454 °C
E_r (°C)	3.06×10^3	275	305	251
P_r (GPa)	7.42	2.80	3.56	2.43
W^{HT}	5.1 μm	1.2 μm	1.1 μm	1.3 μm
W	12.7 μm	6.8 μm	11.9 μm	8.6 μm

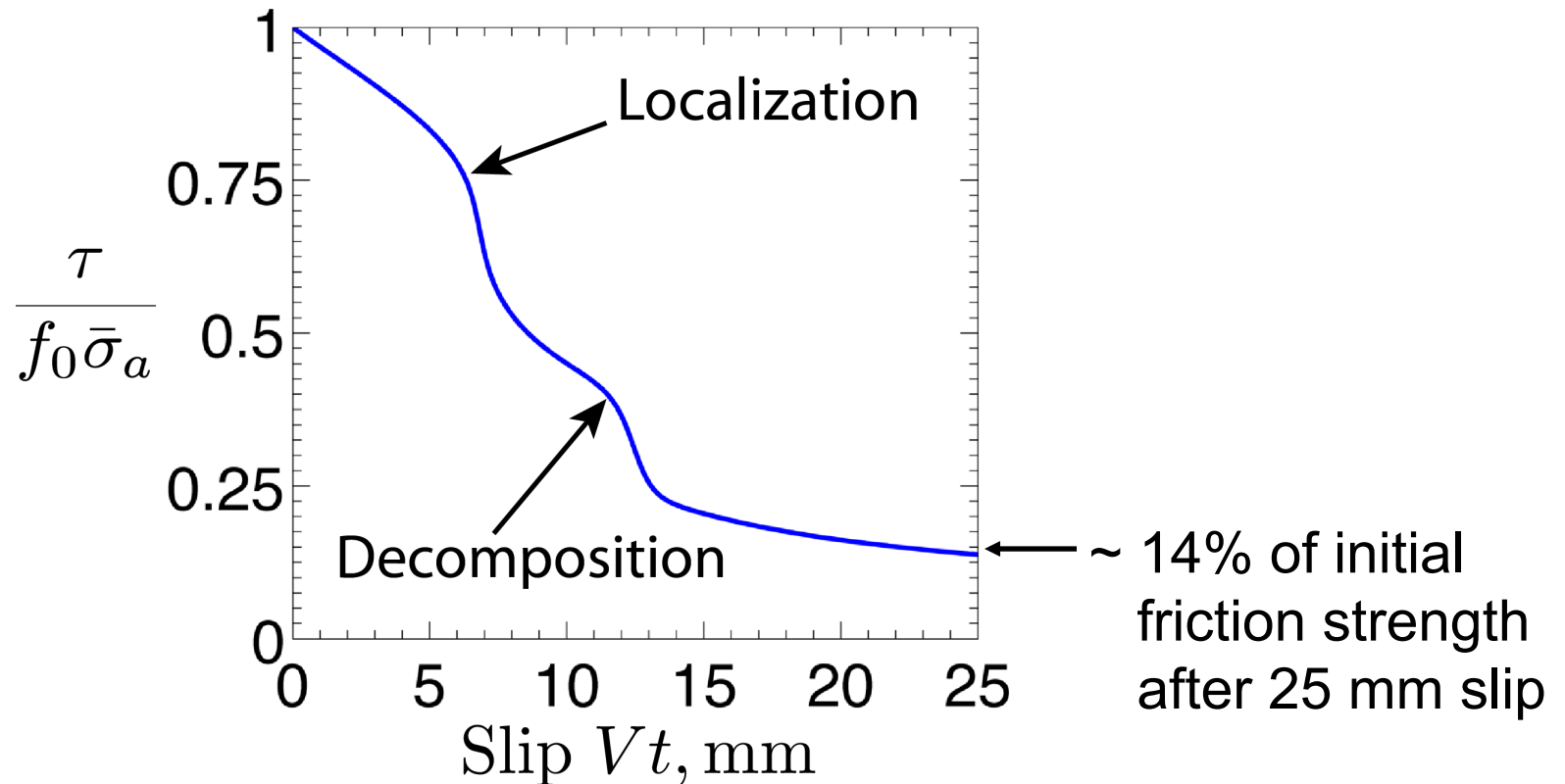
Linear perturbation estimates, localization zone widths :

High T , fast reaction rate limit:
$$W^{HT} \approx \pi^2 \frac{\alpha_{hy}}{V} \frac{(a-b)}{f_o^2} \frac{\rho c E_r}{P_r}$$

Low T , pre-reaction thermal press.:
$$W \approx \pi^2 \frac{a-b}{f_o^2} \frac{\rho c}{\Lambda} \frac{\alpha_{th} + \alpha_{hy}}{V}$$

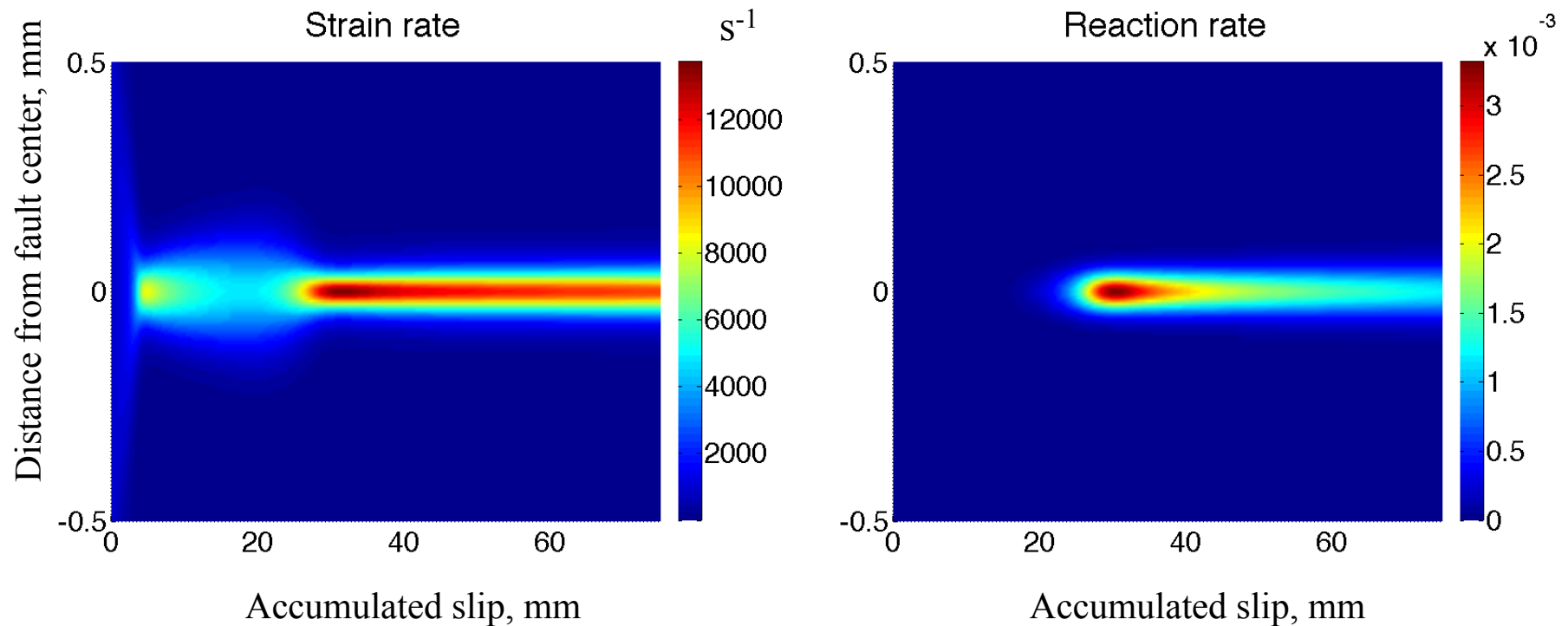
[$W = \lambda / 2$, where λ = longest wavelenth for stable linearized response to infinitesimal $\exp(2\pi i y / \lambda)$ perturbation]

Representative simulations:
thermal pressurization of in-situ fluids,
followed by thermal decomposition



**Suggests faults may be *strong* but *brittle*
(quickly lose strength after slip is initiated
at a place of localized stress concentration)**

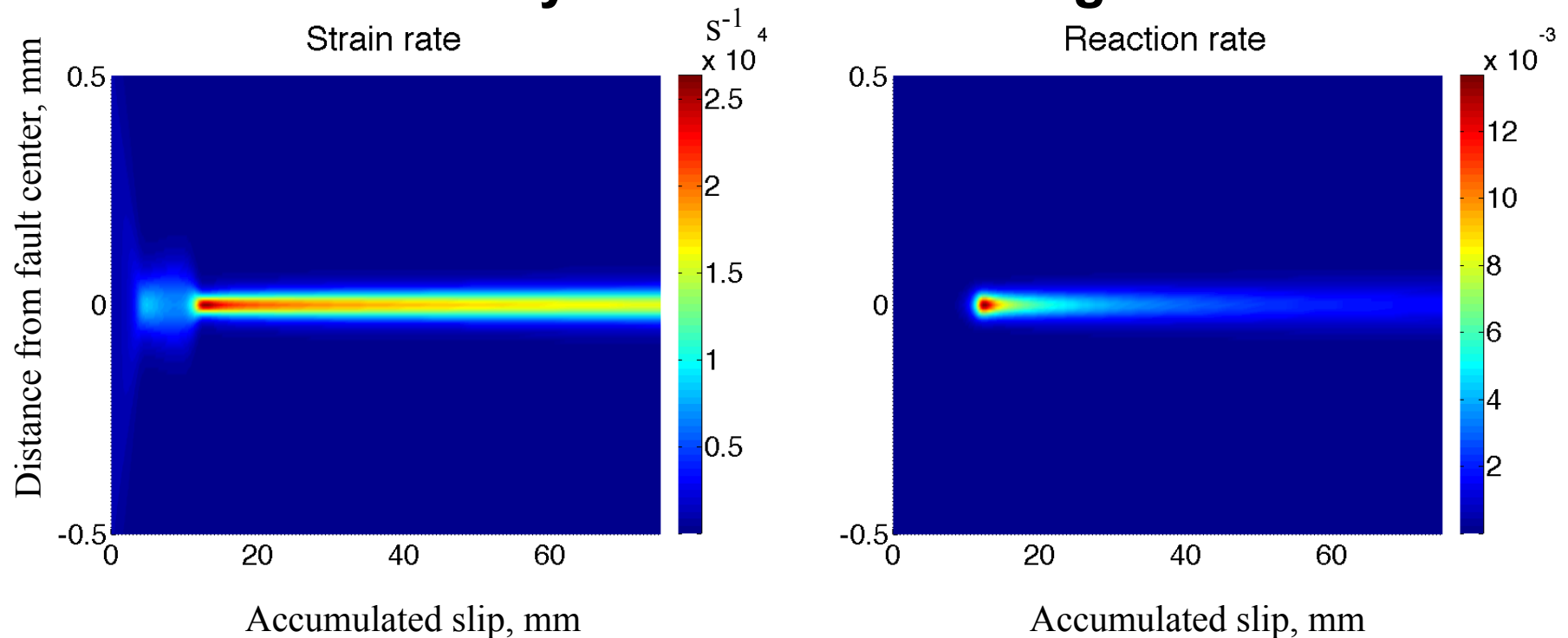
- Numerical solutions for a 1 mm wide gouge layer.



- When the reaction becomes important, we observe significant strain localization ($W_{\text{nonlin. calc.}}$ of order $\sim 2 \times W_{\text{lin. pert.}}$).

Independence of reaction rate

- Our linear stability analysis predicts the localized zone width is independent of kinetic parameters. To test this we **increase A by three orders of magnitude.**

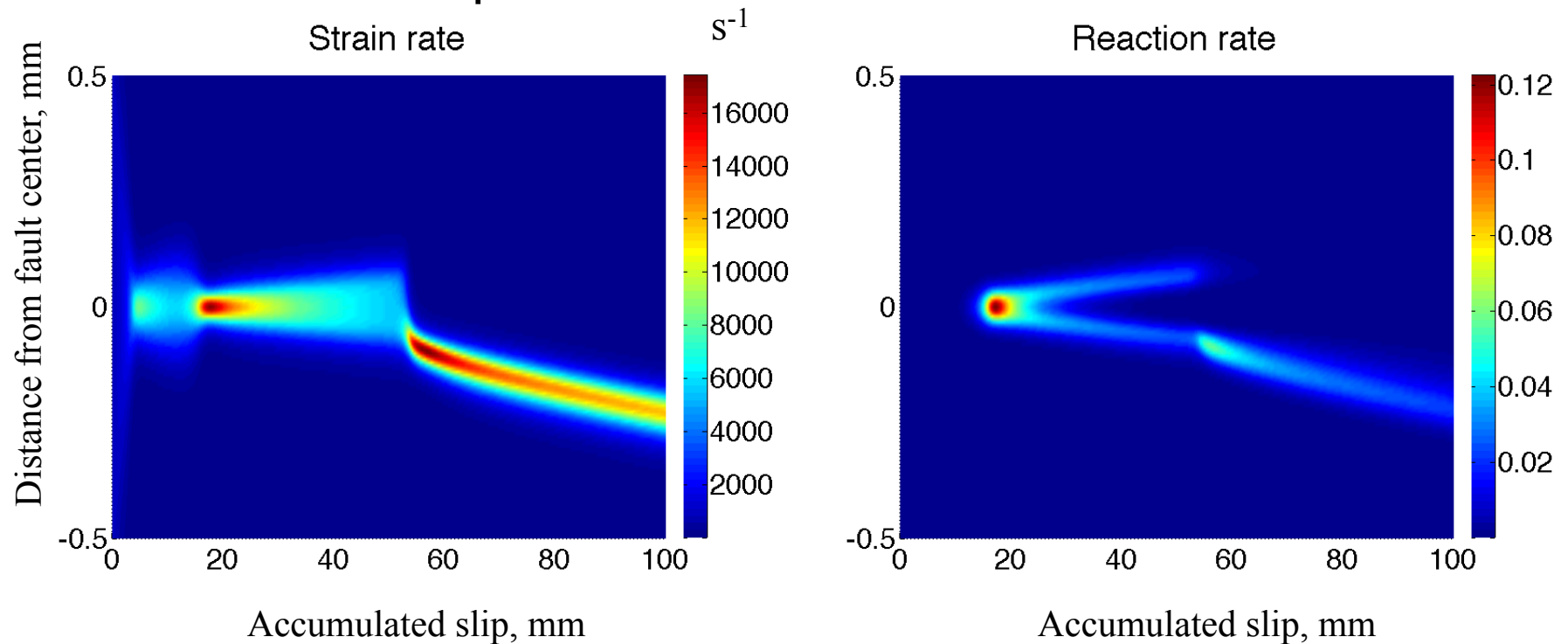


- The localized zone width has only decreased by a factor of two.

Platt, Brantut & Rice (AGU, Fall 2011; in prep 2014 for *JGR*)

Localized zone migration

- Now we investigate a case for which **depletion of reactant** is important.

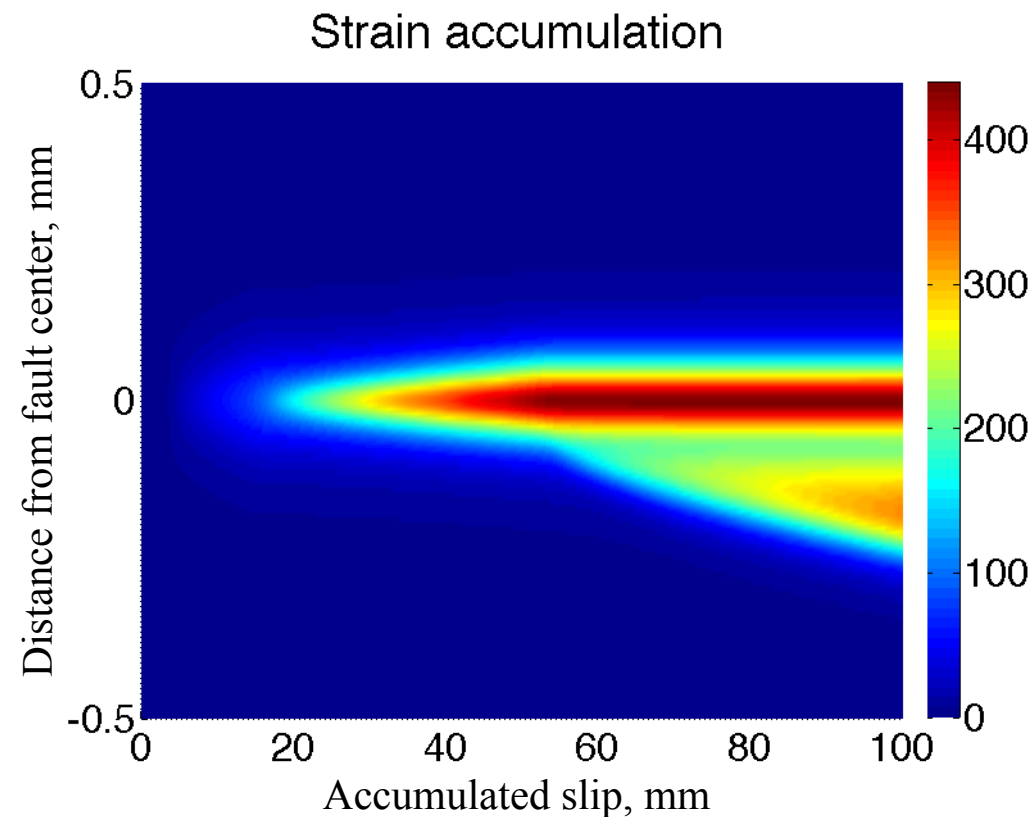


- Depletion causes the zone of localized straining to migrate. The strain rate and reaction rate profiles are strongly coupled.

Platt, Brantut & Rice (AGU, Fall 2011; in prep 2014 for *JGR*)

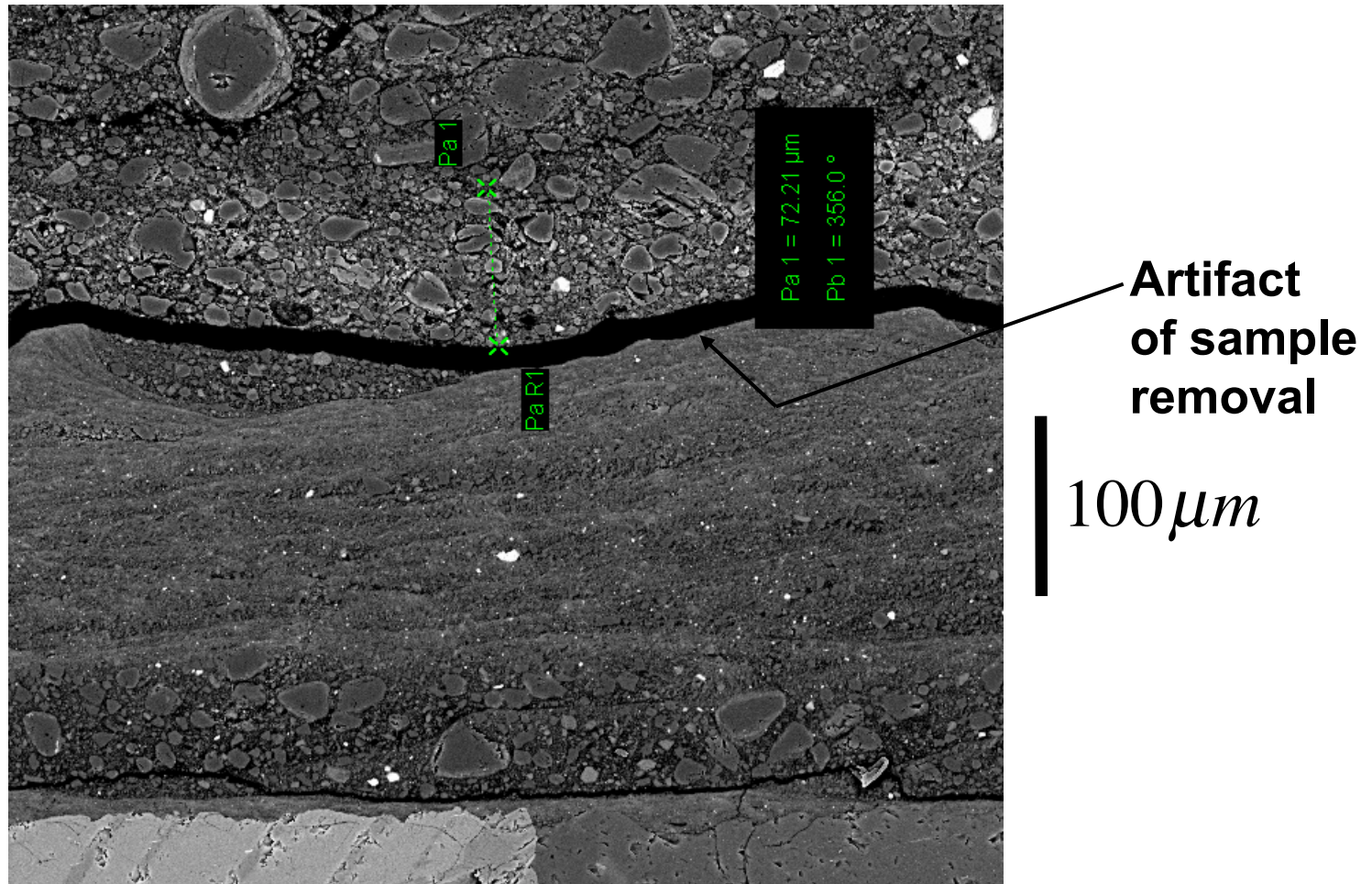
Localized zone migration

- This localized zone migration leads to a complex, non-monotonic, strain history.



Platt, Brantut & Rice (AGU, Fall 2011; in prep 2014 for *JGR*)

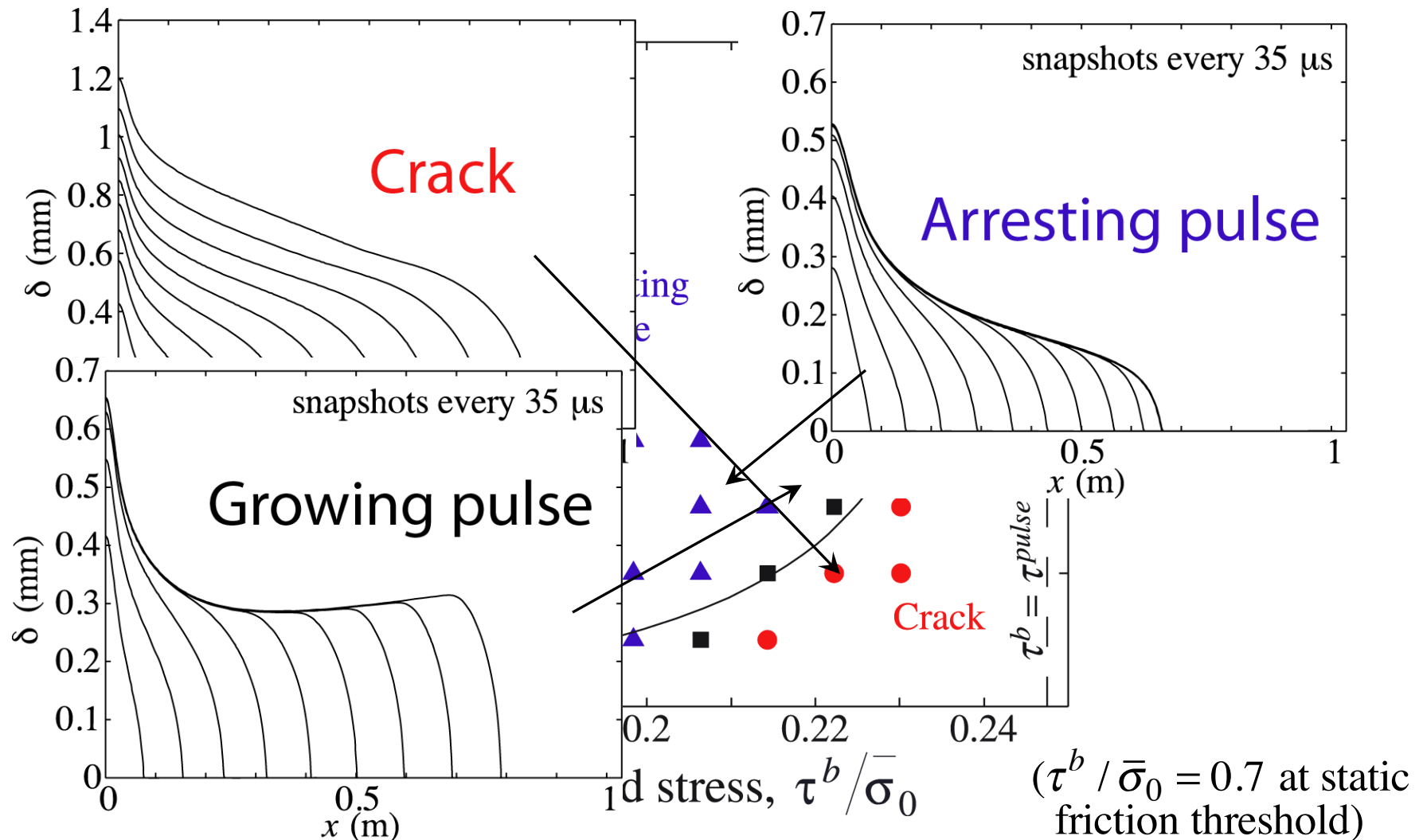
Observation suggesting migration (in rotary shear of carbonate sample)



from T. Mitchell, Univ. Col. London (*private comm.*)

Noda, Dunham & Rice (JGR, 2009)

Effect of strong dynamic weakening (thermal pressurization + flash heating/weakening of frictional contacts) on when a rupture, once nucleated, can propagate to a large spatial extent.



Conclusions

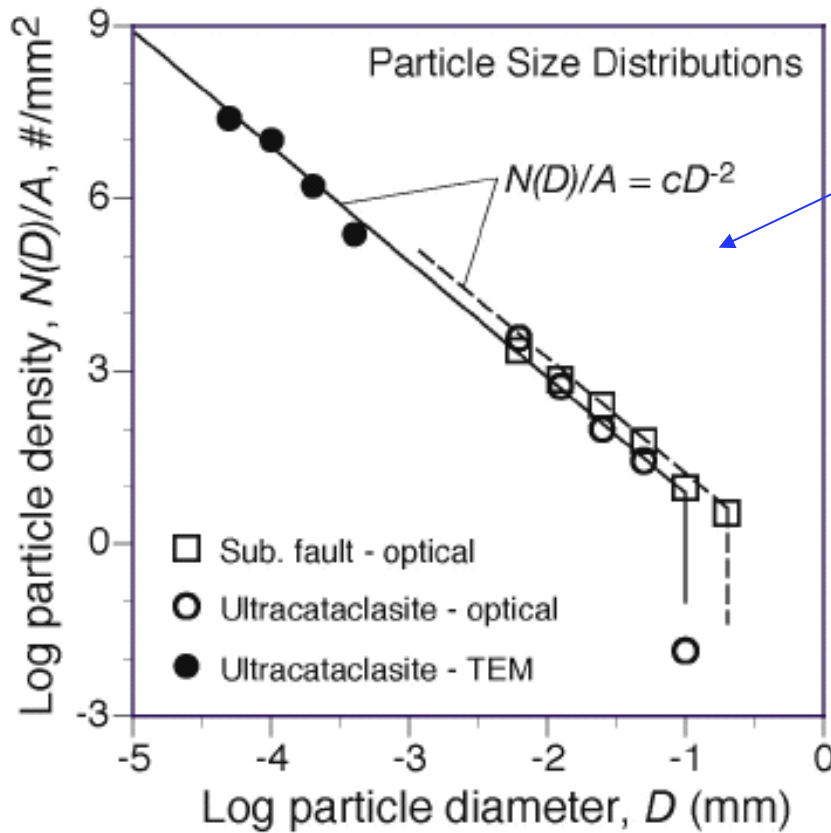
- **Thermal Pressurization of Fluid (Water) Present In-Situ**
 - Linear stability analysis predicts very thin slip zones, width $W \approx 5 - 200 \mu\text{m}$, within observed range.
 - Full nonlinear analysis also predicts very thin slip zones independent of initial layer thickness.
 - Localization causes additional weakening consistent with “slip on a plane” analysis

- **Thermal Pressurization by Decomposition Fluid**
 - Localization to comparable zones , $W \approx 2 - 180 \mu\text{m}$ width
 - Simulations indicated progress of reaction triggers localization
 - Width of localized zone is independent of kinetic parameters.

- **For a wide range of representative parameters, both processes lead to slip on very narrow zones (within the range of observations) causing additional dynamic weakening**

Fault zones undergoing seismic slip:

- Frictional heating leads to dynamic pressurization of pore fluids (native ground fluids, or decomposition products from clays and carbonates) within fault gouge.
- Result is that dramatic shear-weakening results.
- Consequences for the dynamics of rupture propagation and earthquake phenomenology:
 - strong but brittle faults,
 - operating at low overall stress,
 - with no pronounced heat outflow,
 - often showing self-healing rupture mode.



*Particle size distribution for
Ultracataclasite gouge
hosting the Punchbowl pss*

[Chester et al., *Nature*, 2005]

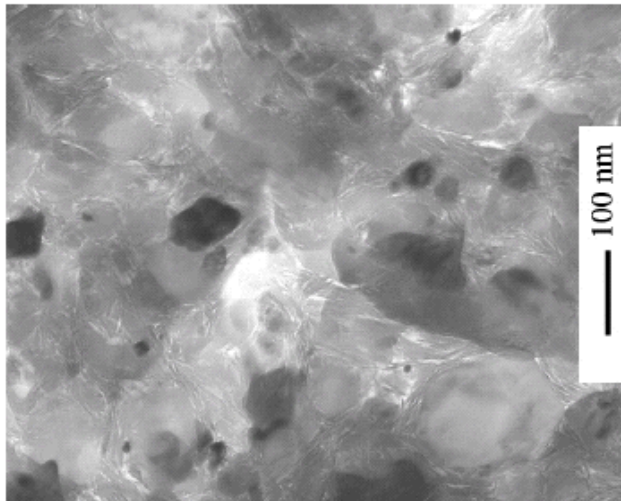
- $N(D) / A =$ number of particles per unit sample area with $2D / 3 < \text{diameter} < 4D / 3$.

- $N(D) / A \approx c / D^2$ for $30 \text{ nm} < D < 70 \text{ }\mu\text{m}$.

In 3D: $\hat{N}(D) / V \approx \hat{c} / D^3$

- D_{50} (= size such that 50% by mass are larger/smaller) $\sim 1 \text{ }\mu\text{m}$.

- Standard granular material guideline (for narrow size range):
thinnest possible shear zone
 $\sim 5 \text{ to } 10 D_{50} \approx 5 \text{ to } 10 \text{ }\mu\text{m}$



New frontier in the elasto-dynamics of spontaneous earthquake rupture:

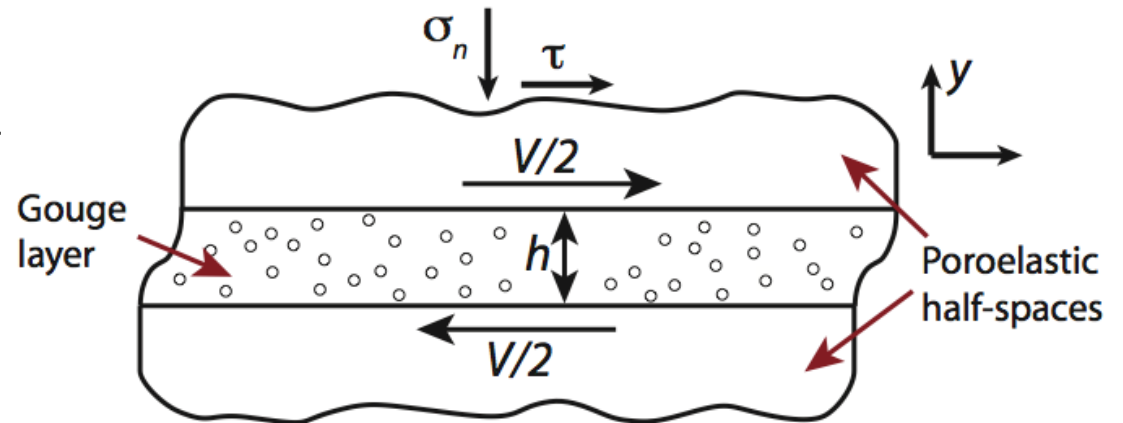
Solve the pde set below at each moment in time, at each point x along a fault zone, to relate the local $\tau(x,t)$ to the local history of $V(x,t)$.

(The $\tau(x,t)$ and $V(x,t)$ are also related by the overall elastodynamics.)

$$\frac{\partial T}{\partial t} = \frac{\tau \dot{\gamma}}{\rho c} + \alpha_{th} \frac{\partial^2 T}{\partial y^2} - E_r \frac{\partial \xi}{\partial t}$$

$$\frac{\partial p}{\partial t} = \Lambda \frac{\partial T}{\partial t} + \alpha_{hy} \frac{\partial^2 p}{\partial y^2} + P_r \frac{\partial \xi}{\partial t}$$

$$\frac{\partial \xi}{\partial t} = A(1 - \xi) \exp\left(-\frac{Q}{RT}\right)$$



GARAGASH: SLIP PULSE WITH THERMAL PRESSURIZATION

(JGR, 2012)

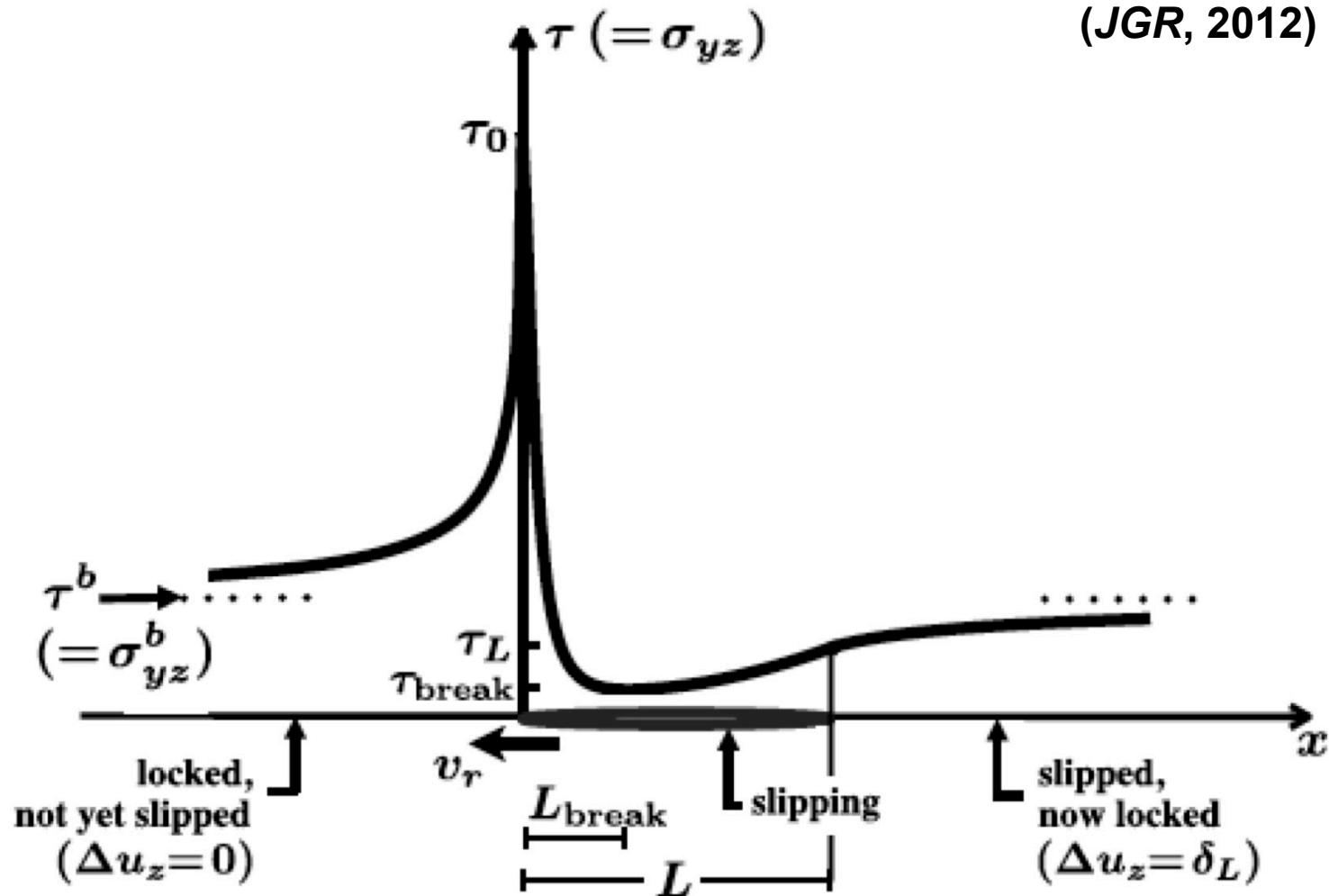


Figure 1. Sketch of a slip pulse and corresponding stress evolution.